Accounting for Point Source Propagation Properties in 3D Fluorescence OPT

A. Darrell, K. Marias, *Member, IEEE*, A. Garofalakis, H. Meyer, Sir Michael Brady, *Senior Member, IEEE*, J. Ripoll.

***Abstract*- Reconstructing 3D images from 2D projections in fluorescence OPT is a relatively new problem requiring attention from researchers in this emerging field. There are several aspects of fluorescence OPT which require different treatment compared with non-fluorescence tomography. One significant problem, and the subject of this paper, is that fluorophores emit light isotropically and so the intensity of light captured at a microscope lens is inversely proportional to the square of the distance of the fluorophore from the focal point of the lens. Standard back-projection techniques do not account for this phenomenon and we show numerically that net effect is that fluorophores close to the centre of a body are assigned relatively low values in standard reconstructions. This is an inherent limitation of the standard back-projection method for quantitative fluorescence applications (e.g. in molecular imaging). In this paper we present a working, though computationally intensive, method to account for this, and discuss how more sophisticated (and less computationally intense) methods could be derived in the near future.**

I. INTRODUCTION

One of the main goals of modern genetics is to link the many thousands of genes identified through genome sequencing of model organisms to gene and protein function. Optical imaging techniques combined with probe development and insertional gene trapping have proved to be invaluable tools for studying functional genomics and proteomics. In specimens such as *Drosophila* however, these advances have so far been limited by the low penetration depth of confocal or epi-fluorescence approaches and therefore the lack of 3D *in vivo* images. Detailed analysis of the distribution of tags or probes is still mostly obtained by means of traditional histology, which excludes the option of performing time-lapse studies on the same subject. However, new optical techniques based on tomographic principles have recently been developed that target a wide variety of tissues ranging from small transparent or semi-transparent samples to whole animals. The past four years has seen the development of Selective Plane Illumination Microscopy (SPIM) [8] - a technique which enables imaging of the interior of small transparent or semi-transparent samples such as zebrafish and *Drosophila* embryos and Optical Projection Tomography (OPT) [3] - a technique used to produce 3D images of transparent tissue samples such as cleared chick embryos. When imaging specimens in the mm to cm range, OPT is the most appropriate technique for obtaining 3D images, both in transillumination and in fluorescence mode. However, due to the fact that fluorophores emit light isotropically, it is not clear that the traditional radon-transform approach is appropriate for reconstructing these images. In this work we present one method to account for the isotropic light emission of fluorophores and propose a new approach to fluorescence OPT.

Manuscript received April 3rd, 2004. This research was supported by E.U. Integrated Project "Molecular Imaging" LSHG-CT-2003-503259. A.D. and H.M. acknowledge support from EST Molec-Imag MEST-CT-2004-007643. J.R. would like to acknowledge very useful discussions with James Sharpe and Miguel Torres.

Alexander Darrell is with Medical Vision Laboratory, Department of Engineering Science, Oxford University, Parks Road, Oxford OX1 3PJ and ICS-FORTH, Vassilika Vouton, P.O.Box 1385, GR 711 10 Heraklion, Greece (email: adarrell@ics.forth.gr).

Kostas Marias was with Medical Vision Laboratory, Department of Engineering Science, Oxford University, Parks Road, Oxford OX1 3PJ. He is now with the ICS-FORTH, Vassilika Vouton, P.O.Box 1385, GR 711 10 Heraklion, Greece (email: kmarias@ics.forth.gr).

Jorge Ripoll, Anikitos Garofalakis and Heiko Meyer are with Institute of Electronic Structure & Laser, Foundation for Research and Technology-Hellas (FORTH) , Vassilika Vouton, P.O.Box 1385, GR 711 10 Heraklion, Greece (email: {jripoll, heimeyer, agarof}@iesl.forth.gr).

Sir Michael Brady is with Medical Vision Laboratory, Department of Engineering Science, Oxford University, Parks Road, Oxford OX1 3PJ, UK. (email: jmb@robots.ox.ac.uk).

II. METHODS

Consider initially, a slice $I(x,y,0), 0 \le x,y \le L$ through a 3D domain $I(x,y,z)$, consisting of a 2D domain containing fluorophore(s). For ease of notation we drop z in the following. For further simplification, consider the case of a single fluorophore situated at position $(X, L/2)$, as in Figure 1. Now consider two projections of this slice, one at 0 degrees and another at 180 degrees (that is, in the $+x$ direction and $-x$ direction). Ignoring scatter, the intensities registered on the detector are given by

$$P(0,\frac{L}{2}) = \frac{F}{(L-X)^2} \tag{1}$$

and

$$P(180,\frac{L}{2}) = \frac{F}{X^2}. \tag{2}$$

F is given by

$$F = I_0 \exp[-\mu_a^{exc} X] \exp\left[-\mu_a^{em}(L-X)\right] \gamma \tag{3}$$

where I_0 is the intensity of the incident excitation radiation, $\mu_a^{exc,em}$ are the absorption coefficients for the excitation and emission radiation, respectively, and γ is the fluorescence cross-section (a product of the quantum yield, the fluorophore concentration and the absorption cross-section of the fluorophore). We make one further simplification, that the excitation and emission absorption coefficients are approximately equal and thus

$$F \approx I_0 \exp[-\mu_a L]\gamma \,. \tag{4}$$

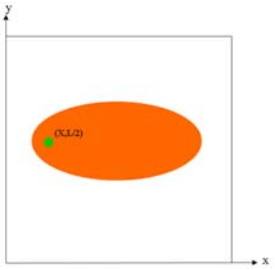


Fig. 1. The contributions of a single fluorophore to opposite projections depend on position. The domain is square of size L by L.

Note that standard back-projection is essentially addition of projections pasted over the image space. Because addition is commutative, opposite pairs of projections could be added first to give a set of quasi-projections over 180 degrees which could in turn be back-projected, giving the same result as simply back-projecting the full set of original projections. Adding the contribution of a fluorophore to opposite projections gives the contribution of that fluorophore to the corresponding quasi-projection, in this case

$$\frac{F}{(L-X)^2}+\frac{F}{X^2}=\frac{F(2X^2+L^2-2XL)}{(L-X)^2X^2}\,. \tag{5}$$

That is, the contribution of a fluorophore to a quasi-projection is weighted according to its perpendicular distance, x, from the edge of the L by L domain by

$$\frac{2x^2+L^2-2xL}{(L-x)^2x^2}\,. \tag{6}$$

So back-projecting an even number of projections taken over the range of 360 degrees from a body containing fluorophores would be equivalent to back-projecting half that number of projections taken over 180 degrees from the same body, in the absence of the isotropical properties of fluorophores, weighting the contribution of each fluorophore by equation (6). Our method therefore is based on reversing this process at the earliest opportunity, when we first obtain a reconstructed image. We take a new set of quasi-projections over 180 degrees from a standard reconstruction (obtained using standard theory [7]), weighting the contribution of each pixel by equation 6, inverted. We then use standard methods to back-project the quasi-projections, thereby obtaining a reconstructed image where the isotropic property of the fluorophores has been accounted for. The implementation of the method and some results, are presented in the next two sections. Figure 2 shows a flowchart which describes the method visually.

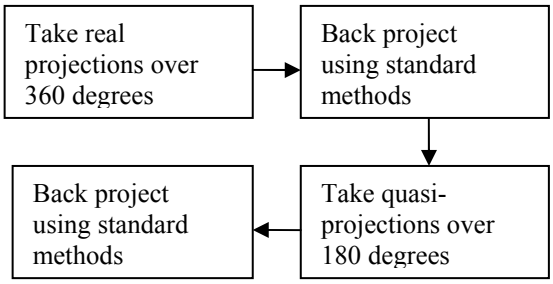


Fig. 2. Flowchart showing the four steps of our method.

III. COMPUTER PHANTOM EXPERIMENTS

Figure 3 shows the computer phantom image used, 500 pixels square, all pixels of value zero except for 6 square regions of pixels, each of side length 20 and value 200 ($\gamma = 200$).

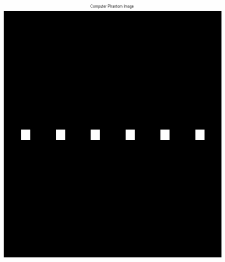


Fig. 3. A 500 by 500 pixel phantom image containing six groups of phantom fluorophores.

For reconstructing the phantom, we computed 500 evenly spaced projections over 360 degrees taking account of fluorophores emitting as point sources while ignoring scatter and absorption (μ_α=0) for I_0 = 1. We used standard methods [7] to back-project the projections and create an initial reconstructed image. Figure 4b shows a bar chart of the mean value assigned for each group of fluorophores in the initial reconstructed image, confirming the effect of using standard back-projection for fluorescence reconstruction in our numerical simulation. The reconstructed image was initially filtered using a 3 by 3 equal value averaging filter for reducing noise, and then took 250 evenly spaced quasi-projections from the resulting image ranging over 180 degrees, weighting the contribution of each pixel by

$$\frac{x^2(L-x)^2}{2x^2+L^2-2xL}\,, \tag{7}$$

where x is the distance from the edge of the L by L domain. Finally, we again used standard back-projection to obtain a

second reconstructed image but this time using the quasi-projections. Figure 4c shows the resulting plot, equivalent to 4a,b.

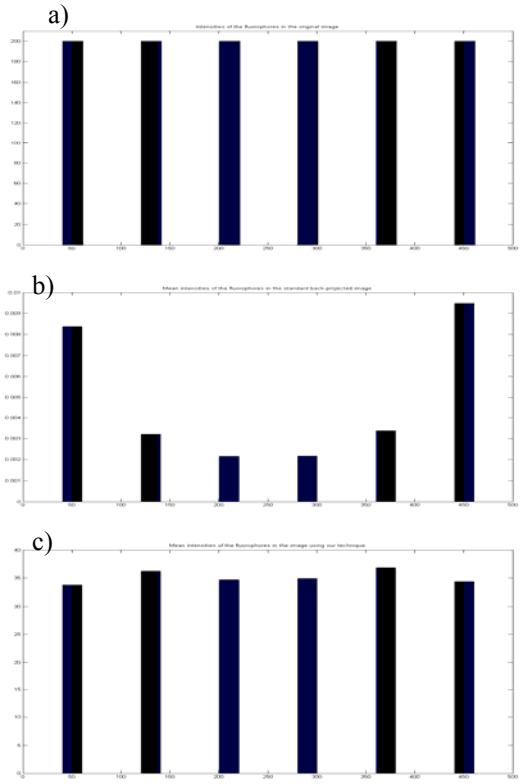


Fig. 4. a) The intensities of the six fluorophores in the original phantom image. b) The mean intensities of the six fluorophores in the image obtained using standard methods. c) The mean intensities of the same fluorophores in the reconstructed image using our method, which accounts for fluorophores emitting as point sources.

It should be noted that neither the image obtained using standard methods, nor the image obtained using our method, in which we attempt to remove the effect of fluorophores emitting light as point sources, report the correct intensities (200) for the six groups of fluorophores. However, our aim at this stage is only to solve the problem caused by the effect of inverse proportionality, which can be summarized by observing that fluorophores of equal intensity in the original image are assigned considerably reduced intensities towards the centre of images acquired using standard back-projection techniques. In this respect, we have clearly made considerable progress, the relatively small differences between intensities in Figure 4c being a subject of further investigation.

IV. PHYSICAL PHANTOM EXPERIMENTS

The phantom used consisted of two hollow glass tubes of 1.8mm internal diameter, each filled with CFSE fluorophore of the same concentration, mounted 10mm apart, one tube positioned at the centre of rotation, the other tube positioned so as to orbit the first during rotation. Excitation light was provided in transmission mode by a cw Ar^{+}-Laser (LaserPhysics, Reliant 1000m, West Jordan, UT 84088 USA) emitting through a custom diffuser consisting of two Perspex sheets mounted 30mm apart and placed between the phantom and the laser. Fluorescence was captured by means of a 40nm bandwidth filter, centered at 540nm (*Chroma Technology Corp., Bellows Falls, VT, 05101 US*) and a 1024x1024 pixel TE-cooled 16bit CCD, cooled to -67^{o}C (Andor Corp., DV 434, Belfast, Northern Ireland). The CCD was equipped with a SIGMA 50mm f/2.8 objective (*Sigma Corporation, Tokyo, Japan*). The phantom (the two tubes filled with fluorophore) was rotated on a motorized rotation stage (model 8MR180, *Standa, Vilnius, Lithuania*) to 360 equally spaced angles over a 360 degree range and projections were taken at each angle. The setup was controlled using custom Labview software. Figure 5 shows a schematic view of the setup.

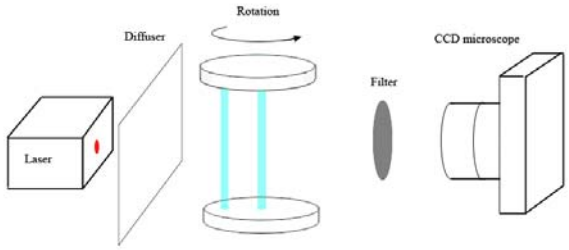


Fig. 5. Schematic view of the phantom and setup used.

Because the phantom used was composed of two parallel tubes mounted vertically and rotated about a vertical axis, each slice (horizontal cross section) of the phantom can be considered identical. Therefore, without loss of generality, the projections of just one slice were considered when testing our reconstruction method. An initial reconstruction was obtained using standard methods [7], see Figure 6 (left). The initial reconstructed image was then filtered using a 3 by 3 equal value averaging filter for reducing artifacts and noise. 180 evenly spaced quasi-projections were taken from the resulting image. Standard back-projection of these quasi-projections resulted in a final image where the mean intensities of the fluorophores were as shown in Figure 6 (right).

V. DISCUSSION

While the method discussed above appears to work both in theory and in practice, the method requires two time consuming iterations of the standard back-projection algorithm and one iteration of our new quasi-projection-taking algorithm. More importantly, the double application

of the back-projection algorithm can be expected to add noise and artifacts thus reducing the quality of the final image.

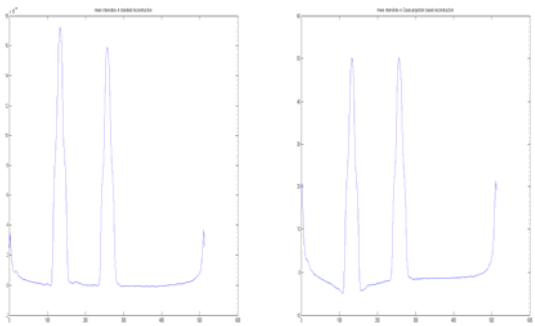


Fig. 6. The mean intensities recorded for the fluorophores in the reconstructed image obtained by standard back-projection (left) and in the reconstructed image obtained by back-projecting quasi-projections (right).

We are working on more sophisticated, potentially quicker methods of dealing with the effect of fluorophores emitting light as point sources/isotropically.

One method we are currently considering can be summarized by observing that while opposite projections describe the same information, the weighting applied to each constituent piece of that information (the inverse squared distance of the information/fluorophore to the edge of the domain) is different for opposite projections and so opposite projections are rarely equal. Conceptually breaking a body into pixel volumes enables the value recorded at each pixel of a CCD camera to be expressed as the product of a row vector of pixel volume values and a column vector of inverse squared distance weightings. For one row of pixels through a body of 100 pixels by 100 pixels, we could obtain two linear equations (one for each of two opposing projections) of 100 unknowns which although impossible to solve for *each* unknown, could be used as a starting point for finding the sum of the unknowns – the sum of fluorescence intensities across the image, without the effect of isotropic light propagation. We have already investigated this in the case where just two pixels in a row contain fluorescence and it leads to a method where the original set of projections taken from a body can be modified to account for point source light propagation, prior to standard back-projection. Extending this method to the general case of an unknown number of fluorophores in an image is the next step and may make use of the differences between each of a full set of projections over 360 degrees rather than just opposite projections.

Another method under consideration involves identifying potential locations of fluorophores in an image space by conceptually back-projecting opposite projections across the image space for each projection angle and assigning at each depth the value a fluorophore would need to have had at that depth in the original body to have given rise to the value recorded at the projection, taking account of inverse squared proportionality. The points at which these opposing back-projections have minimum difference can be considered potential locations of fluorophores in the original body.

We expect our work in the general area of reconstructing 3D OPT images to lead a much fuller understanding of the whole process and possibly an alternative reconstruction algorithm to that offered by the inverse radon approach.

V. REFERENCES

[1] Johnathon R Walls, John G Sled, James Sharpe and R Mark Henkelman, “Correction of Artefacts in Optical Projection Tomography”. Phys. Med. Biol. 50 (2005) 4645-4665.

[2] James Sharpe, Ulf Ahlgren, Paul Perry, Bill Hill, Allyson Ross, Jacob Hecksher-Serensen, Richard Baldock, Duncan Davidson, “Optical Projection Tomography as a Tool for 3D Microscopy and Gene Expression Studies”. Science, vol 296, page 541, April 2002.

[3] James Sharpe, “Optical Projection Tomography”, Annu. Rev. Biomed. Eng. 2004. 6:209-28, April 9, 2004.

[4] Mark Fauver, Eric J. Seibel, J. Richard Rahn, Michael G. Meyer, Florence W. Pattern, Thomas Neumann and Alan C. Nelson, “Three-dimensional imaging of single isolated cell nuclei using optical projection tomography”. Optics Express 4210, Vol 13, No. 11, 30th May 2005.

[5] V. Ntziachristos, J. Ripoll, L.V. Wang, and R. Weissleder, "Looking and Listening to Light: The Evolution of Whole-Body Photonic Imaging". Nat Biotechnol, 23. 313-20 (2005).

[6] K. Marias, J. Ripoll, H. Meyer, V. Ntziachristos, and S. Orphanoudakis, "Image Analysis for Assessing Molecular Activity Changes in Time-Dependent Geometries". IEEE Trans Med Imaging, 24. 894-900 (2005).

[7] A. Kak and M. Slaney, Principles of Computerized Tomographic Imaging, Vol. (IEEE Press, New York, 1988).

[8] Huisken J, Swoger J, Del Bene F, Wittbrodt J, Stelzer EHK. Optical sectioning deep inside live embryos by selective plane illumination microscopy
Science 305: 1007-1009 (2004).